ELSEVIER

Thermochimica Acta 286 (1996) 263–296

thermochimica acta

The application of modulated differential scanning calorimetry to the glass transition of polymers. I. A single-parameter theoretical model and its predictions

J.M. Hutchinson [a,*], S. Montserrat [b]

[a] *Department of Engineering, Aberdeen University, Fraser Noble Building, King's College, Aberdeen AB9 2UE, UK*

[b] *Departament de Màquines i Motors Tèrmics, Universitat Politècnica de Catalunya, Carrer de Colom 11, 08222 Terrassa, Spain*

Received 4 January 1996; accepted 29 February 1996

Abstract

A single relaxation time model describing the kinetics of enthalpy relaxation has been applied to modulated differential scanning calorimetry (MDSC) in the glass transition region. The model is able to describe semi-quantitatively all the characteristic features of MDSC: the average or total heat capacity which is very similar to the conventional DSC response at the same average heating rate; a phase angle between heating rate and heat flow modulations which passes through a maximum in the transition region; a "loss heat capacity" which shows a similar behaviour to the phase angle; and a "storage heat capacity" which shows a sigmoidal change from glassy to liquid-like C_p.

The model is used to predict the effects of the experimental and material parameters. Of the experimental parameters, the most important are the average heating rate and the period. The former affects significantly only the total heat capacity, and in the same way as in conventional DSC. The latter affects significantly only the storage heat capacity, causing the sigmoidal transition to shift to higher temperatures as the period is reduced. The amplitude of temperature modulation appears to have no significant effect within a reasonable range.

These predictions, and those for the effects of some material parameters, namely the initial enthalpic state and the non-linearity parameter, are discussed in the light of published experimental data.

Keywords: Differential scanning calorimetry (DSC); Enthalpy relaxation; Single relaxation time model; Modulated differential scanning calorimetry (MDSC)

* Corresponding author.

PII: S0040-6031(96)02967-X

1. Introduction

The idea of modulating the constant heating rate of conventional differential scanning calorimetry (DSC) was originally conceived by Reading [1–3][1] and was subsequently commercialised by TA Instruments [4] as Modulated Differential Scanning Calorimetry (MDSC). The basic principle is to superimpose upon the constant heating rate of conventional DSC a periodically (and in practice sinusoidally) varying modulation.

Following this commercialisation by TA Instruments, other equipment manufacturers have developed their own variants upon this theme, involving differences in the methods of modulation and analysis. These variants include Dynamic DSC (DDSC) from Perkin-Elmer and Alternating DSC (ADSC) from Mettler Toledo, described in more detail below, as well as Oscillating DSC (ODSC) from Seiko Instruments.

The result of the controlled modulation of the heating rate, by whichever technique, is a periodically varying heat flow, measured by the instrument. This measured heat flow can be analysed in a number of ways, and the different equipment manufacturers use different approaches, discussed further in a later section. However, there appears to be a certain consensus, in that all approaches require a Fourier transformation of the periodically varying heating rate and heat flow data. In particular, such transformation of MDSC data yields two components [1–3] of the heat flow ("reversing" and "non-reversing") and a phase angle between heating rate and heat flow, in addition to a so-called "underlying" or "total" heat flow. These four MDSC output quantities show characteristic features in the glass transition region of polymers, also seen in DDSC [5], which may be summarised as follows:

(i) the underlying heat flow appears similar to the conventional DSC scan, at constant heating rate equal to the average heating rate of MDSC, showing, for example, the usual endotherm associated with enthalpy relaxation;
(ii) the reversing component of the heat flow usually shows a sigmoidal change at an apparent glass transition temperature, T_g(rev), from glassy to liquid-like behaviour, without any endothermic enthalpy relaxation peak;
(iii) the non-reversing component of the heat flow shows a peak in the region of T_g(rev);
(iv) the phase angle also shows a peak in the region of T_g(rev), very similar to the non-reversing component.

The interpretation of some of these features has hitherto remained rather obscure, and on occasion even seems somewhat confused. For example, the observation that T_g(rev), the glass transition temperature found from the reversing component of the

[1] These three journal references followed earlier conference presentations, respectively: J.C. Seferis, I.M. Salin, P.S. Gill and M. Reading, Characterisation of Polymeric Materials by Modulated Differential Scanning Calorimetry, Academy of Athens, Greece, 26 November 1992; P.S. Gill, S.R. Sauerbrunn, B.S. Crowe and M. Reading, Separating Rapidly Reversible and Non-Rapidly Reversible Thermal Transitions by DSC, 10th ICTA Congress, Hatfield, UK, 24–28 August, 1992; M. Reading and V. Hill, MDSC; a New Thermal Method for Characterising Materials, 10th ICTA Congress, Hatfield, UK, 24–28 August 1992.

heat flow, is essentially independent of the average heating rate[2] has prompted the idea of a rate-independent T_g, in contradiction to all current theories of the glass transition [1]. Similarly confusing interpretation has been made of the non-reversing component of the heat flow, which is considered by some authors [3] not to display the glass transition, but to represent the enthalpy relaxation. It is difficult to reconcile this view with the observation of a peak in the non-reversing component not only on heating but also on cooling, for which there is clearly no prior enthalpy relaxation [6].

The problem lies in there being until now no satisfactory theoretical analysis to describe the above characteristic features resulting from the kinetics of the response of the sample to the modulations of heating rate in the glass transition interval. Theoretical analyses to date either have considered only the effects of heat transfer, and hence of temperature differences between block, sample and reference [7, 8] or have introduced a kinetic response in a rather arbitrary way, ignoring non-linear effects [6, 9, 10]. Thus, although these analyses can, for example, describe the phase shift between sample and reference temperatures in the steady state when the heat capacity is constant [7], they cannot account for the usually observed features of the MDSC response in the glass transition interval because they do not contain the appropriate kinetic response of the sample.

This problem was recognised by Wunderlich et al. [7], who suggested an approach based upon the hole theory of Hirai and Eyring [11, 12]. We present here an alternative approach, based upon the single-parameter version [13] of the multiparameter KAHR model [14], which has successfully been applied in the analysis and interpretation of conventional DSC data. It will be shown first that this model can describe all of the common features of MDSC, and then the model will be used to predict the effects of the various experimental and material parameters on the MDSC data. In the second paper in this series [5], these theoretical predictions will be compared with experimental data from the (approximately equivalent) technique of DDSC. A further paper will examine the extension of the theoretical analysis from the single-parameter model to the multi-parameter model.

2. Theory

2.1. Heating rate modulation

2.1.1. Modulated DSC

In MDSC, the temperature T is programmed to follow a sinusoidal modulation, of amplitude A_T and frequency ω (radians s^{-1}), around a constant rate of increase (or decrease) of temperature, q_{av}, from an initial temperature T_o, so that the time (t)

[2] It is a misconception, unfortunately quite widely held, that the glass transition temperature may be obtained from a DSC heating scan. The glass transition temperature is defined on *cooling* from the equilibrium liquid to the glassy state, and is a function of cooling rate. What one can obtain from the heating scan is a fictive temperature, which is not usually the same as the glass transition temperature.

dependence is

$$T = T_o + q_{av}t + A_T \sin(\omega t) \tag{1}$$

The heating (or cooling) rate q is therefore given by

$$q = q_{av} + A_T\omega \cos(\omega t) \tag{2}$$

from which it can be seen that q is modulated cosinusoidally around an average rate, q_{av}, with an amplitude $A_q = A_T\omega$ and with the same frequency, ω, as the temperature modulation. Alternatively, one could describe the modulation in terms of the period of the cycle, per, given by $\text{per} = 2\pi/\omega$, and hence there is an alternative relationship between the amplitudes of temperature and heating rate modulations, namely $A_q = A_T\omega = A_T 2\pi/\text{per}$. The heating rate is therefore completely defined by three variables (q_{av}, A_T, ω), all of which can be varied independently. This is illustrated schematically in Fig. 1a.

In these cycles, any given temperature may be passed either only once or more than once, depending on the relative values of these variables. For example, the first critical condition, involving the change from a temperature being encountered once to three times (twice on heating, once on cooling), occurs when the heating rate first becomes negative, i.e. part of the cycle involves cooling, and may be described by

$$q_{av} = 2\pi A_T/\text{per} \tag{3}$$

The next critical condition (any temperature being encountered five times; three times on heating and twice on cooling) may be shown to occur when

$$\sqrt{1 + \left(\frac{3\pi}{2}\right)^2}\, q_{av} = 2\pi A_T/\text{per} \tag{4a}$$

or approximately

$$q_{av} = 2\pi A_T/(4.8\,\text{per}) \tag{4b}$$

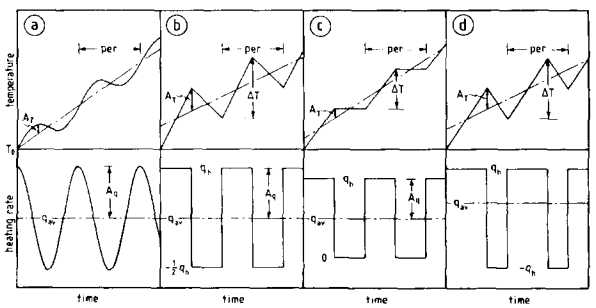

Fig. 1. Schematic illustration of the modulations of temperature and heating rate during heating for the various techniques considered: (a) modulated DSC; (b) dynamic DSC, heat–cool mode; (c) dynamic DSC, heat–iso mode; (d) alternating DSC, cycles for envelope analysis. A_T = amplitude of temperature modulation; A_q = amplitude of heating rate modulation; per = period of modulation cycle; q_{av} = average heating rate. For DDSC and ADSC: ΔT = temperature increment on heating; q_h = heating rate.

With typical values of A_T and per, it is not difficult for q_{av} to exceed this latter critical value (Eq. (4b)). However, to restrict MDSC cycles to "heating only", in other words maintaining q_{av} greater than the former critical value, defined by Eq. (3), as is sometimes advocated [10], imposes some limitations on the ranges of experimental variables that can be used. For example, it is usually considered necessary to have a minimum number of cycles (say 10) through the width of any transition (say 15°C); under these circumstances, maintaining "heating only" cycles would require the amplitude of the temperature modulation to be less than 0.24°C [= width/(number of cycles × 2π)].

2.1.2. Dynamic DSC

In DDSC (Perkin-Elmer) the temperature programme may be of two types, heat–cool and heat–iso modes, described in the following sections.

Heat–cool mode

Here the temperature varies in a saw-tooth manner, with the duration of the heating stage equal to the duration of the cooling stage. In general, the temperature will increase by an amount ΔT_1 at constant heating rate and then decrease by an amount ΔT_2 at an appropriate constant cooling rate, with a total period for the cycle defined by per. The heating rate modulation will be of the square-wave form, with an average heating rate given by

$$q_{av} = \frac{\Delta T_1 - \Delta T_2}{\text{per}} \tag{5}$$

and the temperature amplitude will be given by

$$A_T = \frac{\Delta T_1 + \Delta T_2}{4} \tag{6}$$

As an example, the temperature could rise by ΔT at heating rate q_h and then decrease by $\Delta T/2$ at cooling rate $-q_h/2$; such cycles are illustrated in Fig. 1b. The amplitude of the temperature modulation is then given by $A_T = 3\Delta T/8$, and the average heating rate is $q_{av} = q_h/4$, so that one may derive, from the relationship between q_h, per and ΔT, namely

$$q_h \,\text{per}\,/2 = \Delta T \tag{7}$$

the relationship between the three experimental variables (q_{av}, per, A_T) for the particular cycles shown in Fig. 1b

$$3\,\text{per}\,q_{av} = 4A_T \tag{8}$$

Consideration of the temperature variation shown in Fig. 1b indicates that in this mode any temperature is encountered three times, twice on heating and once on cooling.

Heat–iso mode

In this mode, the temperature increases at rate q_h for a temperature interval ΔT, and then remains constant (isothermal) for an equal length of time to the heating ramp (see Fig. 1c). The heating rate modulation is again of the square-wave form, with a minimum heating rate of zero.

Relationships between the variables can again be defined, but in this case, unlike the general form of the heat–cool mode, the three experimental variables are not independent. The amplitude of temperature modulation is $A_T = \Delta T/4$, and the average heating rate is $q_{av} = q_h/2$, while Eq. (7) still holds for the relationship between q_h, per and ΔT. Thus one finds

$$\text{per}\, q_{av} = 4A_T \tag{9}$$

One can also show that, for both heat–cool and heat–iso modes, the amplitude of the heating rate modulation is related to the amplitude of the temperature modulation by $A_q = 4A_T/\text{per}$.

2.1.3. Alternating DSC

In ADSC (Mettler Toledo), the temperature profile, and therefore also the heating rate profile, can be selected as required; for example, any one cycle can be composed of up to 40 segments of temperature ramps. For the so-called "envelope analysis", a saw-tooth temperature waveform is used, similar to that for DDSC, but here the temperature increases at rate q_h for an interval ΔT, and then decreases at an equal and opposite rate $-q_h$ for half the interval, $\Delta T/2$. Thus the cooling stage has duration only half that of the heating stage, and the heating rate modulation is square-wave, but asymmetric, unlike both MDSC and DDSC (see Fig. 1d).

The inter-relationships here are: $A_T = \Delta T/3$ and $q_{av} = q_h/3$, but now Eq. (7) becomes

$$q_h\, \text{per} = 3\Delta T/2 \tag{10}$$

so that one may write

$$2\, \text{per}\, q_{av} = 3A_T \tag{11}$$

It should be noted that it is difficult to define an amplitude for the heating rate modulation as this profile is asymmetric (see Fig. 1d), which would have important consequences for the later Fourier transformation of the ADSC output data. For these purposes, therefore, it would be best to select the temperature profile to give a symmetric heating rate modulation.

2.2. Enthalpy relaxation kinetics

The single parameter model is introduced in order to describe the kinetics of enthalpy relaxation during the rather complex thermal histories illustrated in Fig. 1, and in particular during MDSC. The basic equation relates the rate of change of excess enthalpy δ (equal to $H - H_\infty$, where H is the specific enthalpy and H_∞ is its value in

equilibrium at the same temperature) to a heating rate term and a relaxation term, as

$$\frac{d\delta}{dt} = -\Delta C_p\, q - \frac{\delta}{\tau(T,\delta)} \tag{12}$$

Here ΔC_p is the difference between the specific heat capacities of the equilibrium liquid (C_{pl}) and of the glass of fixed structure (C_{pg}), i.e. of constant fictive temperature T_f, and τ is the (single) relaxation time, which depends upon both temperature (T) and structure (δ). This equation has been used previously [13] to describe the response of glasses in conventional DSC. It is recognised that, being a single-parameter model, it does not include the well-known feature that relaxation processes in glasses involve a distribution of relaxation times (or may be described by a non-exponential process). This feature will be included in a later paper, by means of the multiparameter KAHR model [14], which will introduce the important aspect of "memory effects"; for the present, though, we retain the simplicity of the single-parameter model in order to describe to a first approximation the response of glasses to MDSC thermal histories.

The dependence of the relaxation time τ upon T and δ is defined by an equation used previously [13, 14]

$$\tau = \tau_g \exp[-\theta(T - T_g)]\exp[-(1-x)\theta\delta/\Delta C_p] \tag{13}$$

In this equation, τ_g is the value of the relaxation time in equilibrium ($\delta = 0$) at an arbitrary glass transition temperature T_g, θ is a parameter defining the temperature dependence of τ and may be related approximately to an apparent activation energy Δh^* ($\theta \approx \Delta h^*/RT_g^2$), and $x(0 \le x \le 1)$ is the non-linearity parameter defining the relative contributions of temperature and structure to the relaxation time. This equation has been shown [15] to be equivalent to the alternative

$$\tau = \tau_0 \exp\left[\frac{x\Delta h}{RT} + \frac{(1-x)\Delta h^*}{RT_f}\right] \tag{14}$$

often referred to as the Tool–Narayanaswamy–Moynihan equation [16–18].

Eq. (12) describes the response of the glass to any prescribed thermal history, defined by q. For example, in MDSC q is given by Eq. (2), while in DDSC and ADSC it is best treated as a sequence of discrete constant-rate heating and cooling (or isothermal) stages. Because for MDSC q can be expressed as a simple algebraic function of time (Eq. (2)), this is the variant that will be analysed further here. It should be noted that this analysis treats only the kinetic response of the glass, and does not include heat transfer effects; in other words, it is assumed that heat transfer to the sample is infinitely good, and that the sample follows exactly the imposed temperature programme. Clearly this is a simplification, but it has been common practice in the description of conventional DSC. Standard temperature calibration routines, as used in conventional DSC, could be adopted in MDSC, though the varying heating rate would make this a considerably more complex procedure, and additionally there are procedures, see, for example, Ref. [19], for making corrections for thermal lag within the sample. For the present, we adopt this simplifying assumption and proceed to the Fourier transform analysis.

2.3. Specific heat capacities

Eq. (12) is solved numerically using a 4th–5th-order Runge–Kutta routine, and the solution is in the form of a time (or temperature) dependence of the excess enthalpy δ. From this, the heat flow, HF, is obtained in one of two equivalent ways

$$\mathrm{HF} = C_{pl}q + \frac{\mathrm{d}\delta}{\mathrm{d}t} \tag{15a}$$

or

$$\mathrm{HF} = C_{pg}q - \frac{\delta}{\tau(T,\delta)} \tag{15b}$$

both of which derive from the heat flow being the time derivative of the enthalpy, and hence related to the time derivative of δ

$$\frac{\mathrm{d}\delta}{\mathrm{d}t} = \frac{\mathrm{d}}{\mathrm{d}t}(H - H_{\infty}) = \mathrm{HF} - \frac{\mathrm{d}H_{\infty}}{\mathrm{d}T}\frac{\mathrm{d}T}{\mathrm{d}t} = \mathrm{HF} - C_{pl}q \tag{15c}$$

Eq. (15b) is derived from Eq. (15a) using Eq. (12).

The usual procedure is to make the Fourier transformation of the periodically varying heating rate and heat flow. Whether or not this is a mathematically justifiable procedure is discussed later; for the present, we adopt common practice and make a cycle-by-cycle Fourier transform of both MDSC heating rate and the heat flow response. That is to say, each cycle of heating rate is Fourier transformed (and being an exact cosinusoid gives predictable values for frequency, amplitude, phase, and d.c. component or average value over the cycle), and the heat flow variation over exactly the same time interval is also Fourier transformed. The heat flow, which in general is not purely sinusoidal, will have contributions with frequencies different from the fundamental frequency of the heating rate modulation. Again in common with usual practice (but discussed further later), only the contribution from the fundamental frequency ω is considered, for which an amplitude and phase angle (of the heat flow, the output or dependent variable of the MDSC, with respect to that of the heating rate, the input or controlled variable of the MDSC), as well as a d.c. component or average value, may be obtained. Thus we can define the following values, adopting the kind of notation used by Wunderlich et al. [7]

$\langle q \rangle$: average heating rate $= q_{\mathrm{av}}$
$\langle \mathrm{HF} \rangle$: average heat flow
A_q : amplitude of heating rate $= A_T\omega$
A_{HF} : amplitude of heat flow
ϕ : phase angle between heating rate and heat flow

Because these Fourier transforms are made for each discrete cycle of heating rate, one value for each of the above five quantities is obtained for each cycle, and these are associated with the average time (mid-period) or average temperature of the cycle. For

MDSC, the average temperature of the cycle occurs at the mid-period; this is not the case for either of the DDSC modes or for ADSC (see Figs. 1b–1d).

In order finally to define specific heat capacities, the approach due to Schawe [6] is used. An average, or "total", specific heat capacity, $\langle C_p \rangle$, is found from the average values of q and HF

$$\langle C_p \rangle = \frac{\langle \mathrm{HF} \rangle}{\langle q \rangle} \tag{16}$$

This is the same definition as used in MDSC [7–10]. From the amplitudes, Schawe derives a "complex" specific heat capacity, C_p^*

$$C_p^* = \frac{A_{\mathrm{HF}}}{A_q} \tag{17}$$

which is the same definition as used in MDSC for the so-called "reversing" heat capacity [7–10]. The difference between Schawe's approach [6] and that of MDSC [7–10] lies in the treatment adopted by Schawe, analogous to that used in dynamic mechanical analysis for example, which is to define storage (C_p') and loss (C_p'') components from the complex specific heat capacity, making use of the phase angle

$$C_p' = C_p^* \cos\phi \tag{18}$$

$$C_p'' = C_p^* \sin\phi \tag{19}$$

It should be noted that the usual MDSC notation of "reversing" and "non-reversing" components does not correspond exactly to the definitions in Eqs. (18) and (19). For small phase angles, the reversing heat capacity, defined as A_{HF}/A_q and hence equal to C_p^*, is approximately equal to C_p' since $\cos\phi \approx 1$ under these conditions. On the other hand, the non-reversing heat capacity, obtained by subtracting the reversing heat-flow component from the total heat flow, is not equal, even approximately, to C_p'' when the phase angle departs from zero, as it does in the transition region. This difference was pointed out by Schawe [6], and for this reason we do not make further reference to non-reversing components.

These definitions (Eqs. (16)–(19)) are used here to derive the various specific heat capacities from the theoretical heat flow found from the solution to the differential equation, Eq. (12). These results, as well as the time and temperature dependence of other more fundamental quantities such as excess enthalpy and heat flow, are presented below.

3. Results

3.1. Initial values

In the numerical analysis presented here, typical values have been chosen for the material parameters, which in fact correspond closely to those obtained experimentally for a fully cured epoxy resin based upon diglycidyl ether of bisphenol A [20]. These are

as follows

$C_{pl} = 1.6\,\mathrm{J\,g^{-1}K^{-1}}$

$C_{pg} = 1.3\,\mathrm{J\,g^{-1}K^{-1}}$

$\Delta C_p = 0.3\,\mathrm{J\,g^{-1}K^{-1}}$

$\theta = 1.0\,\mathrm{K^{-1}}$

$x = 0.4$ (except for the evaluation of the effect of x)

$\tau_g = 100\,\mathrm{s}$

The value of θ corresponds approximately to an apparent activation energy $\Delta h^* = 1200\,\mathrm{kJ\,mol^{-1}}$ for $T_g = 105°\mathrm{C}$.

The temperature scale is made with reference to an arbitrary T_g at which the relaxation time in equilibrium is 100 s. All the simulated MDSC scans start from $T_o = T - T_g = -20\,\mathrm{K}$, and end at $T - T_g = 10\,\mathrm{K}$ after passing through the transition region.

The initial value of the excess enthalpy δ at T_o before the start of the MDSC simulation is usually $\delta_o = 6\,\mathrm{J\,g^{-1}}$. This value corresponds to an instantaneous quench from equilibrium at T_g to T_o. More realistically, it also corresponds to cooling at a constant rate of approximately $-20\,\mathrm{K\,min^{-1}}$ from equilibrium at 10 K above T_g, with $x = 0.4$ as above.

In Sections 3.2 below, the response of the model in respect of excess enthalpy, heat flow and the various specific heat capacities is presented for a typical combination of the MDSC experimental variables, namely

$q_{av} = 2.5\,\mathrm{K\,min^{-1}}$

$\mathrm{per} = 24\,\mathrm{s}$

$A_T = 0.25\,\mathrm{K}$

In Sections 3.3 that follow, the effects of the various parameters—the experimental variables q_{av}, per and A_T, as well as the material parameter x and the initial condition δ_o—on the MDSC response will be examined in turn.

3.2. *Response of the model*

3.2.1. *Excess enthalpy*

An illustration of a typical variation of the excess enthalpy during an MDSC run is shown in Fig. 2, together with the corresponding conventional DSC result for the same values of the material parameters and experimental variables. The general shape of the curve shows the usual overshoot where δ passes to negative values before approaching equilibrium at higher temperature. This overshoot is a necessary event under all conditions, as equilibrium on heating must be approached from negative values of δ [14].

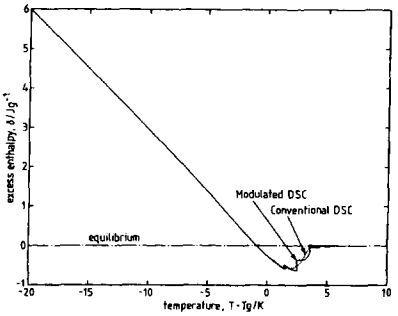

Fig. 2. Excess enthalpy modulation in MDSC with per = 24 s, $q_{av} = 2.5\,K\,min^{-1}$, $A_T = 0.25\,K$, $\delta_o = 6\,J\,g^{-1}$ and $x = 0.4$. The horizontal dash-dotted line represents equilibrium ($\delta = 0$). The full line represents the MDSC response; the dotted line represents the conventional DSC response. A full line is used where the two responses overlap, approximately in the temperature range up to $T - T_g = 0\,K$ and for $T - T_g > 5\,K$. Refer to Fig. 18 for more detail in the temperature range from $T - T_g = 0$ to $T - T_g = 6\,K$.

It can be seen that the difference between MDSC and conventional DSC becomes significant only in this overshoot region, and is confined to a temperature interval of about 5 K. In fact, the narrowness of this interval is a result of the present analysis using only a single-parameter model; a distribution of relaxation times would broaden the response.

The effect of the heating rate modulations is clearly seen in this interval, where δ is rather irregularly modulated around the conventional DSC response. The modulated response actually appears to reach an equilibrium state ($\delta = 0$) at a temperature well below that for conventional DSC (see Fig. 18 (below) for an expanded view), but then departs again from equilibrium because the heating rate reaches a value too great to maintain this equilibrium. Indeed, this occurs in two successive cycles before the MDSC and DSC traces become indistinguishable at higher temperature.

3.2.2. Heat flow modulation

Once the time or temperature dependence of δ has been established (e.g. Fig. 2), the heat flow modulation can be calculated from Eqs. (15a) or (15b). A typical result is shown in Fig. 3a and b, for the temperature and time dependences respectively, using the same values of experimental variables as for Fig. 2.

It can be seen from Fig. 3a that the particular combination of q_{av}, per and A_T chosen here results in a looping of the heat flow because the heating rate becomes negative for part of the cycle, i.e. q_{av} is less than the critical value defined by Eq. (3).

The heat flow envelope described by Fig. 3a shows constant, but different, amplitudes above and below the transition region, with a rather complex response over the same rather narrow temperature interval for which δ departed significantly from the conventional DSC response in Fig. 2.

The envelope of the time dependence (Fig. 3b) also shows this change in amplitude, with the transition occurring approximately in the time interval between 500 and 600 s,

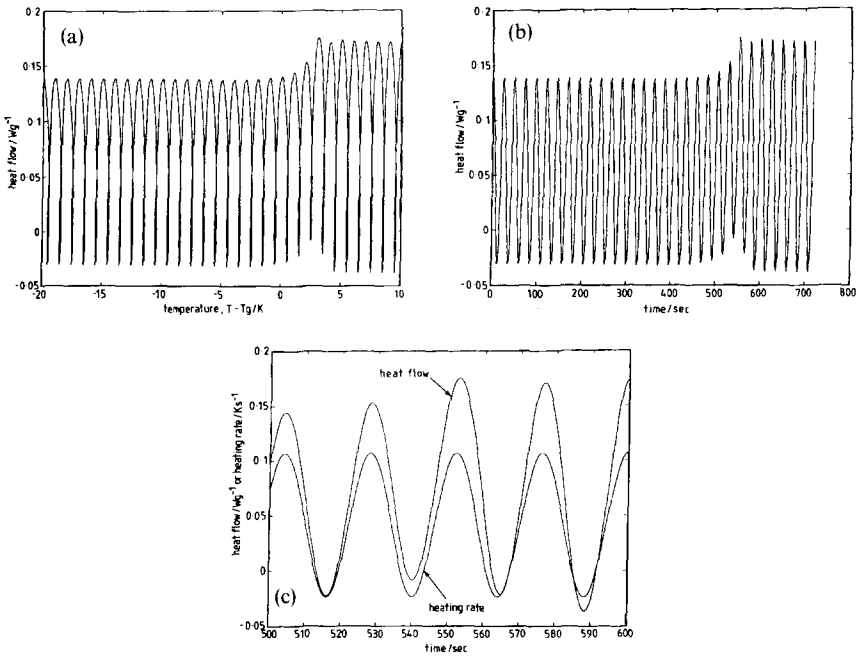

Fig. 3a and b. Modulation of heat flow as a function of temperature (a), and time (b), for the same values of experimental variables as for Fig. 2. Fig. 3c. Modulations of heating rate and heat flow from Fig. 3b on an expanded scale in the transition interval. Note that the units of heating rate are K s^{-1} here so that the same scale can be used for both heating rate and heat flow.

involving four or five cycles. At first glance, these heat flow modulations appear to be very regularly spaced along the time axis, but if this transition interval is expanded (see Fig. 3c), and compared with the heating rate modulation in this interval, an important difference can be seen. The first two cycles of heating rate and heat flow in this time interval appear closely in phase, as do the fourth cycles; the third cycles, however, show a clear displacement on the time axis. It is this effect which, when the cycles are Fourier transformed, gives rise to the phase angle ϕ.

3.2.3. *Average heat capacity, $\langle C_p \rangle^*$*

The average, or "total", heat capacity $\langle C_p \rangle$ is found from the Fourier-transformed cycles of Fig. 3b using Eq. (16), and the results are shown in Fig. 4 as the open circles. Each point corresponds to the Fourier-transformed data from a single cycle of heating rate and the corresponding cycle of heat flow. Also shown, as the full line, is the model simulation of a conventional DSC scan with the same conditions, i.e. with a constant heating rate of 2.5 K min^{-1}, equal to q_{av} for the MDSC scan, and with an initial condition $\delta_o = 6\,J\,g^{-1}$ at $T_o = T_g - 20\,K$. It can be seen that the conventional and modulated DSC results are very similar, though there is a small difference at temperatures just above that of the endothermic peak.

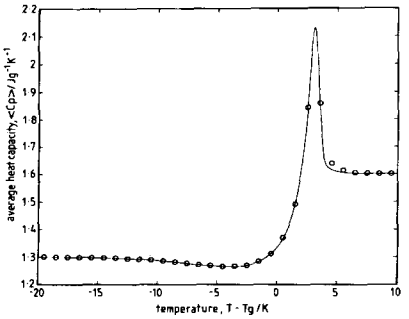

Fig. 4. Average or "total" C_p obtained from MDSC cycles with q_{av}, per, A_T, δ_0 and x the same as for Fig. 2 (open circles). The full line corresponds to the simulation of conventional DSC with heating rate equal to q_{av}.

3.2.4. *Phase angle* ϕ

The dependence of the phase angle ϕ on temperature is found for the Fourier-transformed cycles of Fig. 3b and is shown in Fig. 5. It can be seen that the heating rate and the heat flow are in phase ($\phi = 0$) at the beginning and end of the MDSC scan, but that in the transition region ϕ departs from zero, in this case by about 0.2 radians. Fig. 3c shows how this phase difference arises, but also shows that the heat flow (the output or dependent variable of the MDSC) lags behind the heating rate (the input or controlled variable of the MDSC). For this reason, the phase angle is shown here as negative in this region, even though it is more common practice to assign positive values to ϕ.

In fact, it can also be seen from Fig. 5 that before the large negative departure of ϕ there is a small positive departure. In other words, the heat flow initially leads the heating rate by a small angle before lagging it by a much greater amount. This small positive departure begins at a temperature close to that at which the excess enthalpy δ overshoots the equilibrium line (see Fig. 2), and then changes to a negative departure at a temperature close to that at which δ takes its minimum value (Fig. 2).

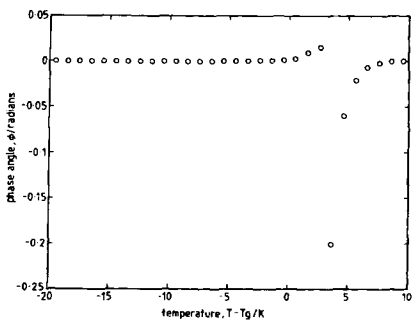

Fig. 5. Phase angle as a function of temperature for MDSC cycles with q_{av}, per, A_T, δ_0 and x the same as for Fig. 2.

3.2.5. *Storage heat capacity*, C'_p

From the phase angle and the complex heat capacity calculated from Eq. (17), the storage heat capacity C'_p is found from Eq. (18), and is shown in Fig. 6. In fact, for small phase angles such as those values shown in Fig. 5, there is little difference between the complex and storage heat capacities ($\cos\phi \approx 1$). C'_p changes rather abruptly from a constant value equal to $C_{pg}(1.3\,\mathrm{J\,g^{-1}K^{-1}})$ in the glassy region to another constant value equal to $C_{pl}(1.6\,\mathrm{J\,g^{-1}K^{-1}})$ in the liquid-like region. The transition occurs over a narrow temperature interval, the same temperature interval as that for which ϕ departs from zero (compare Fig. 5).

Close inspection of this transition shows in fact that the model predicts a small peak in C'_p before it reaches the constant value of C_{pl} at higher temperature. This feature will be seen to be more marked when other experimental conditions are considered (see below).

3.2.6. *Loss heat capacity*, C''_p

Similarly to C'_p, the loss heat capacity is found from the phase angle and C^*_p, using Eq. (19), and is shown in Fig. 7. When ϕ is small, as is the case here, $\sin\phi \approx \phi$ and the dependence of C''_p on temperature is very similar to that of the phase angle. In particular, it shows a small positive departure and then a rather larger negative departure from equilibrium, in the same transition interval of temperature as for ϕ and C'_p, with a value of zero for the glassy and liquid-like region. The negative values are simply a result of the sign convention adopted here for the phase angle, though it should be noted that for the opposite (more usual) sign convention this model still predicts small negative values for the loss heat capacity, in the temperature range just below its maximum departure.

3.3. *Effects of experimental variables*

In the results presented above, a single set of parameter values was chosen in order to illustrate the general features of the model simulations. In the sub-sections that follow

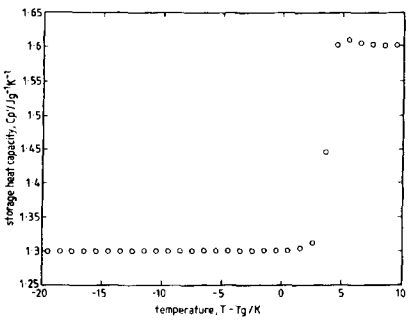

Fig. 6. Storage heat capacity C'_p as a function of temperature for MDSC cycles with q_{av}, per, A_T, δ_0 and x the same as for Fig. 2.

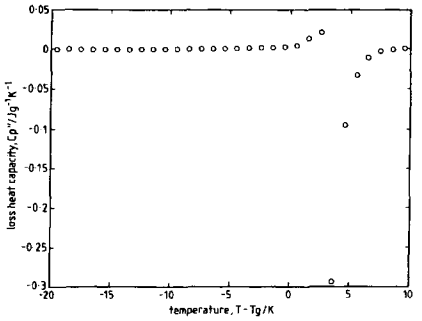

Fig. 7. Loss heat capacity C_p'' as a function of temperature for MDSC cycles with q_{av}, per, A_T, δ_o and x the same as for Fig. 2.

here, each of the experimental variables is considered in turn in order to examine its effect on the MDSC response.

3.3.1. Effect of average heating rate

The response of the model for the conditions per = 24 s, $A_T = 0.5$ K, $\delta_o = 6$ J g^{-1} and $x = 0.4$ has been examined for a number of average heating rates, q_{av}.

For a very slow rate, $q_{av} = 0.625$ K min^{-1}, the average temperature rises by only 0.25 K per cycle, and a large number of cycles (120 in this case) is required to cover the temperature range from $T_g - 20$ K to $T_g + 10$ K. This can be seen in Fig. 8, which shows the heat flow as a function of temperature. The small shoulder seen in the upper envelope results from the very different timescales for the underlying heating rate and

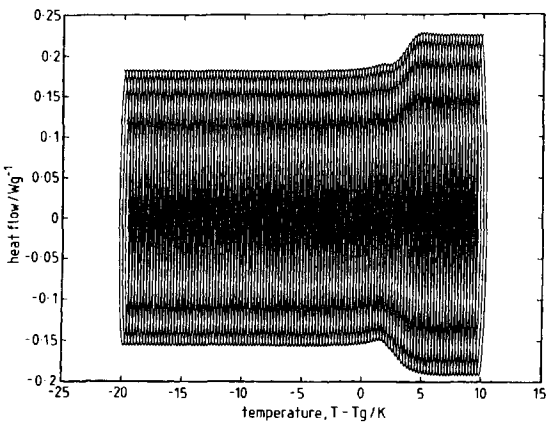

Fig. 8. Cyclic heat flow as a function of temperature for MDSC cycles with per = 24 s, $A_T = 0.5$ K, $\delta_o = 6$ J g^{-1}, $x = 0.4$ and $q_{av} = 0.625$ K min^{-1}.

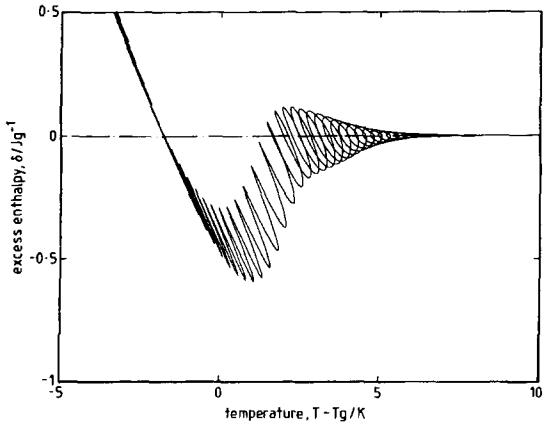

Fig. 9. Variation of excess enthalpy as a function of temperature for MDSC cycles with per = 24 s, $A_T = 0.5$ K, $x = 0.4$, $\delta_o = 6$ J g^{-1}, $x = 0.4$ and $q_{av} = 0.625$ K min^{-1}. The equilibrium ($\delta = 0$) line is shown dash-dotted. Note the expanded temperature scale.

for the periodic modulations. In conventional DSC at the same heating rate of 0.625 K min^{-1}, equilibrium would be established ($\delta = 0$) at about $T - T_g = 2$ K. This temperature, though, is too low for the glass to remain in equilibrium at the limits of the heating rate modulation ($+8.48$ K min^{-1} and -7.23 K min^{-1}), and hence the response departs from what would have been equilibrium in conventional DSC. Furthermore, this departure includes both positive and negative δ, as both cooling and heating rates are involved, and is clearly seen in Fig. 9 which illustrates the cyclic variation of the excess enthalpy δ. As a consequence, the average heat capacity $\langle C_p \rangle$ shows a number of spurious maxima and minima in the temperature range between about $T - T_g = 2$ K and the establishment of a true equilibrium just above $T - T_g = 5$ K. However, the phase angle and the storage and loss heat capacities, derived from the amplitudes of the modulations, display their usual characteristic behaviours.

With increasing q_{av}, the shoulder in the upper envelope (determined by the average heating rate) moves towards higher temperature, while the small peak in the upper envelope (determined by the constant frequency of these cycles) remains essentially invariant at about $T - T_g = 5$ K. The shoulder and peak begin to merge at approximately $q_{av} = 2.5$ K min^{-1}, and, with increasing q_{av}, what was previously only a shoulder develops into a dominant peak. This is illustrated in Fig. 10 for $q_{av} = 7.5$ K min^{-1}. As would be expected, the average specific heat capacity $\langle C_p \rangle$ passes through a maximum at increasingly higher temperatures as q_{av} increases, but the phase angle and the loss heat capacity C_p'' now, for $q_{av} = 7.5$ K min^{-1}, show significant positive as well as negative departures from zero, while the storage heat capacity no longer shows just a sigmoidal change but displays also a more and more pronounced peak. An illustration of this latter effect is given in Fig. 11.

The effect of q_{av} on the average heat capacity, $\langle C_p \rangle$, is shown in Fig. 12 for a smaller temperature amplitude of 0.25 K and with the same values as above for per, δ_o and x.

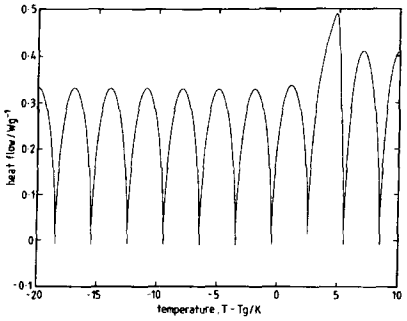

Fig 10. Variation of heat flow with temperature for MDSC cycles with per = 24 s, $A_T = 0.5$ K, $x = 0.4$, $\delta_0 = 6$ J g^{-1}, and $q_{av} = 7.5$ K min^{-1}.

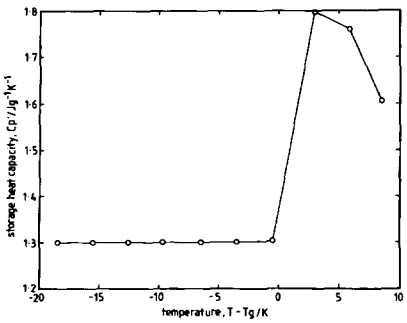

Fig. 11. Variation of storage heat capacity C'_p as a function of temperature during MDSC cycles with per = 24 s, $A_T = 0.5$ K, $x = 0.4$, $\delta_0 = 6$ J g^{-1}, and $q_{av} = 7.5$ K min^{-1}. This should be compared with Fig. 6 for which a smaller average heating rate was used. Note that the lines are drawn simply to join the points, and have no further significance.

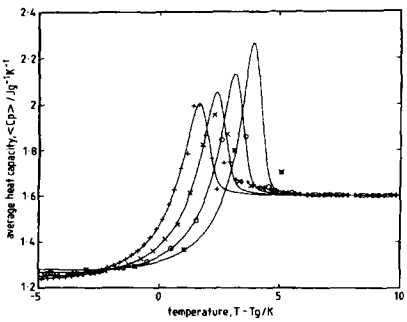

Fig. 12. Variation of the average specific heat capacity as a function of temperature for MDSC cycles with $A_T = 0.25$ K, per = 24 s, $\delta_0 = 6$ J g^{-1}, and $x = 0.4$, for the different average heating rates indicated: +, 0.625 K min^{-1}; x, 1.25 K min^{-1}; ○, 2.5 K min^{-1}; *, 5 K min^{-1}. The full lines represent the response of the model in conventional DSC for the same heating rates. Note the expanded temperature scale and the increasing "undershoot" as the average heating rate is reduced.

Also included in this figure are the curves obtained by modelling conventional DSC at the same (constant) heating rates. It should be noted that, while the agreement between the conventional DSC response and the MDSC response for $\langle C_p \rangle$ is generally very good, there are noticeable differences in the temperature range close to and just above the endothermic peak for each scan. These differences appear particularly marked at the highest heating rate for which there are very few cycles here, and at the lowest heating rate, for which spurious maxima in the temperature range just above the endothermic peak were noted earlier when the temperature amplitude was greater (0.5 K).

3.3.2. Effect of period

Changing the period of the MDSC cycles has a complementary effect on the heat flow to changing q_{av}. This is illustrated in Fig. 13, which represents the heat flow for MDSC cycles with $q_{av} = 2.5\,\mathrm{K\,min^{-1}}$ and per = 12 s, while the other parameters take the same values as for Fig. 8. Comparing Figs. 8 and 13, it can be seen that the same shoulder and small peak occur in the upper envelope, but that in Fig. 13 they are both displaced to higher temperatures. The shoulder is displaced because it corresponds to the effect of q_{av}, which was shown above to move to higher temperatures as q_{av} is increased. The small peak, or more precisely the transition between the constant small amplitude and the constant large amplitude of the envelope, corresponds to the period, and the comparison of Figs. 8 and 13 therefore shows that the effect of decreasing the period is to displace this transition towards higher temperatures.

This can be seen particularly clearly if the storage heat capacity, C'_p, is considered. Designating a mid-point temperature, T_{mid}, as the temperature at which the value of C'_p is mid-way between the glassy ($1.3\,\mathrm{J\,g^{-1}K^{-1}}$) and liquid-like ($1.6\,\mathrm{J\,g^{-1}K^{-1}}$) values, the dependence of T_{mid} on period is shown in a semi-logarithmic plot in Fig. 14. On

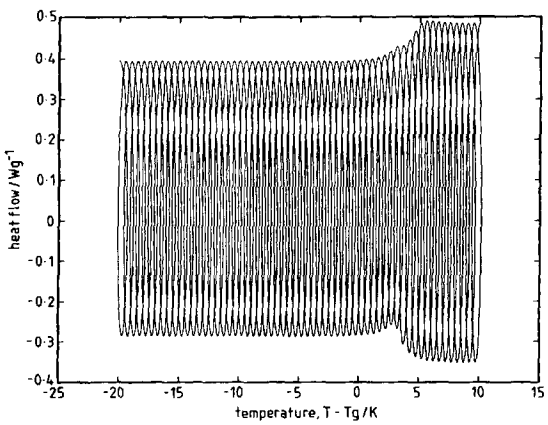

Fig. 13. Cyclic heat flow as a function of temperature for MDSC cycles with per = 12 s, $A_T = 0.5$ K, $x = 0.4$ and $q_{av} = 2.5\,\mathrm{K\,min^{-1}}$.

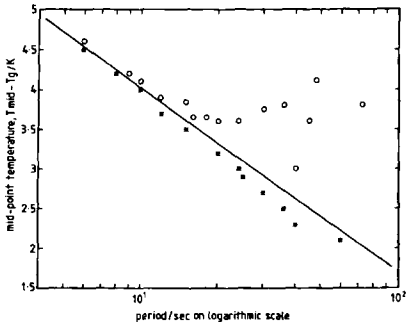

Fig. 14. Dependence of T_{mid} on period for MDSC cycles with $q_{av} = 2.5\,K\,min^{-1}$, $\delta_o = 6\,J\,g^{-1}$, $A_T = 0.25\,K$, and $x = 0.4$. Open circles show results obtained from heating curves (q_{av} positive); stars show results obtained from cooling curves (q_{av} negative). The full line is drawn with slope given by $\theta = 1.0\,K^{-1}$.

heating, T_{mid} decreases approximately linearly with log(period) up to a period of about 24 s, but for longer periods there is a large scatter in the results. This scatter may be attributed to the significant amount of enthalpy relaxation which occurs during one cycle within the glass transition interval, which distorts the heat flow wave form from sinusoidal; the Fourier transform of this distorted waveform is rather sensitive to the selection of the start and end points of the cycles.

On cooling, however, the linear decrease of T_{mid} with increasing log(period) is much better defined, extending over the full range of periods used here. The decrease of approximately 2.5 K as the period increases by one decade is a significant amount, and the effect has been seen experimentally in DDSC [21]. The reason for this dependence is simple. During the course of an MDSC heating scan, the relaxation time τ (compare Eq. (13)) decreases overall as a function of time or temperature, though of course there are cyclic variations. An example is shown in Fig. 15 for the same MDSC parameter values as were used to obtain the heat flow modulations shown in Fig. 13, for which in particular the period was 12 s. When the period is short compared with τ, e.g. at

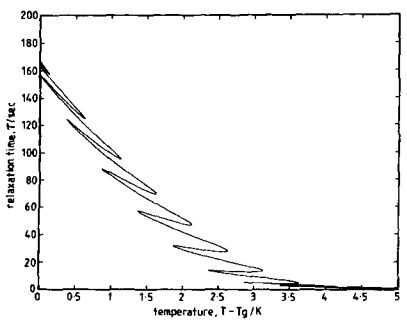

Fig. 15. Dependence of relaxation time τ on temperature for MDSC cycles in which per = 12 s, $A_T = 0.5\,K$, $q_{av} = 2.5\,K\,min^{-1}$, $\delta_o = 6\,J\,g^{-1}$, and $x = 0.4$. Note the expanded temperature scale.

$T - T_g = 0$ in Fig. 15, the response will be glassy as there is no time during the cycle for any significant relaxation to occur. When the period is long compared with τ, e.g. at $T - T_g > 5\,K$ in Fig. 15, the structure of the sample will follow the temperature modulations, giving in this case a liquid-like response. Thus, in the corresponding heat flow modulations in Fig. 13, the envelope gives a glassy C'_p at $T - T_g = 0$ and a liquid-like C'_p at temperatures above $T - T_g = 5\,K$. Between these temperatures, there is a transition from glass to liquid, the exact form of which depends on the other MDSC parameter values.

Since the relaxation time is given by Eq. (13), the approximation that T_{mid} occurs when per $= \tau$ can lead to a theoretical dependence for T_{mid} on period. If the effect of structure (δ) on τ is ignored by neglecting the second exponential term in Eq. 13, one can write

$$\frac{d(T_{mid} - T_g)}{d\log(per)} = -\frac{2.303}{\theta} = -2.303 \tag{20}$$

and a line with this slope is included in Fig. 14. It can be seen that the slope corresponds quite well with the numerical data, with any discrepancy (both in the slope and in the absolute location of this line) being attributed to the simplifying neglect of the structural term, i.e. the second exponential term, in Eq. (13).

3.3.3. *Effect of amplitude*

The effect of the amplitude of the temperature modulation (on the periodically varying heat flow) is shown for MDSC cycles with per $= 24\,s$, $q_{av} = 2.5\,K\,min^{-1}$, $\delta_o = 6\,J\,g^{-1}$ and $x = 0.4$ in the series of Figs. 16a–16f, representing values of A_T increasing from 0.1 to 1.0 K, as indicated in the caption.

The average heat capacity, $\langle C_p \rangle$, obtained from the Fourier transformation procedure is very similar to that for conventional DSC for A_T up to about 0.6 K. For amplitudes greater than this, differences between $\langle C_p \rangle$ and the conventional DSC response appear, particularly in the region of the endothermic peak. For example, Fig. 17 shows both $\langle C_p \rangle$ (circles) and the conventional C_p (full line) for $A_T = 1.0\,K$, where it can be seen that MDSC greatly overestimates the "correct" peak value of approximately $2.1\,J\,g^{-1}K^{-1}$. The reason for this is that the large amplitude of temperature modulation corresponds also to a large amplitude of heating rate modulation; in particular, the maximum heating rate for the cycles represented by the MDSC data in Fig. 17 is $18.2\,K\,min^{-1}$, which gives rise to a peak in the heat capacity much larger than that expected for a heating rate of only the average value of $2.5\,K\,min^{-1}$, and very similar to the maximum value ($2.8\,J\,g^{-1}K^{-1}$) for conventional DSC at $18.2\,K\,min^{-1}$ (compare dashed line in Fig. 17), though occurring at a noticeably different peak temperature. The amplitude of temperature modulation must therefore be somewhat restricted if the $\langle C_p \rangle$ from MDSC is to be considered as equivalent to C_p from conventional DSC.

Below this limiting value of A_T (about 0.6 K in the present instance with the parameter values stated above), the effect of the amplitude can be seen as an approxi-

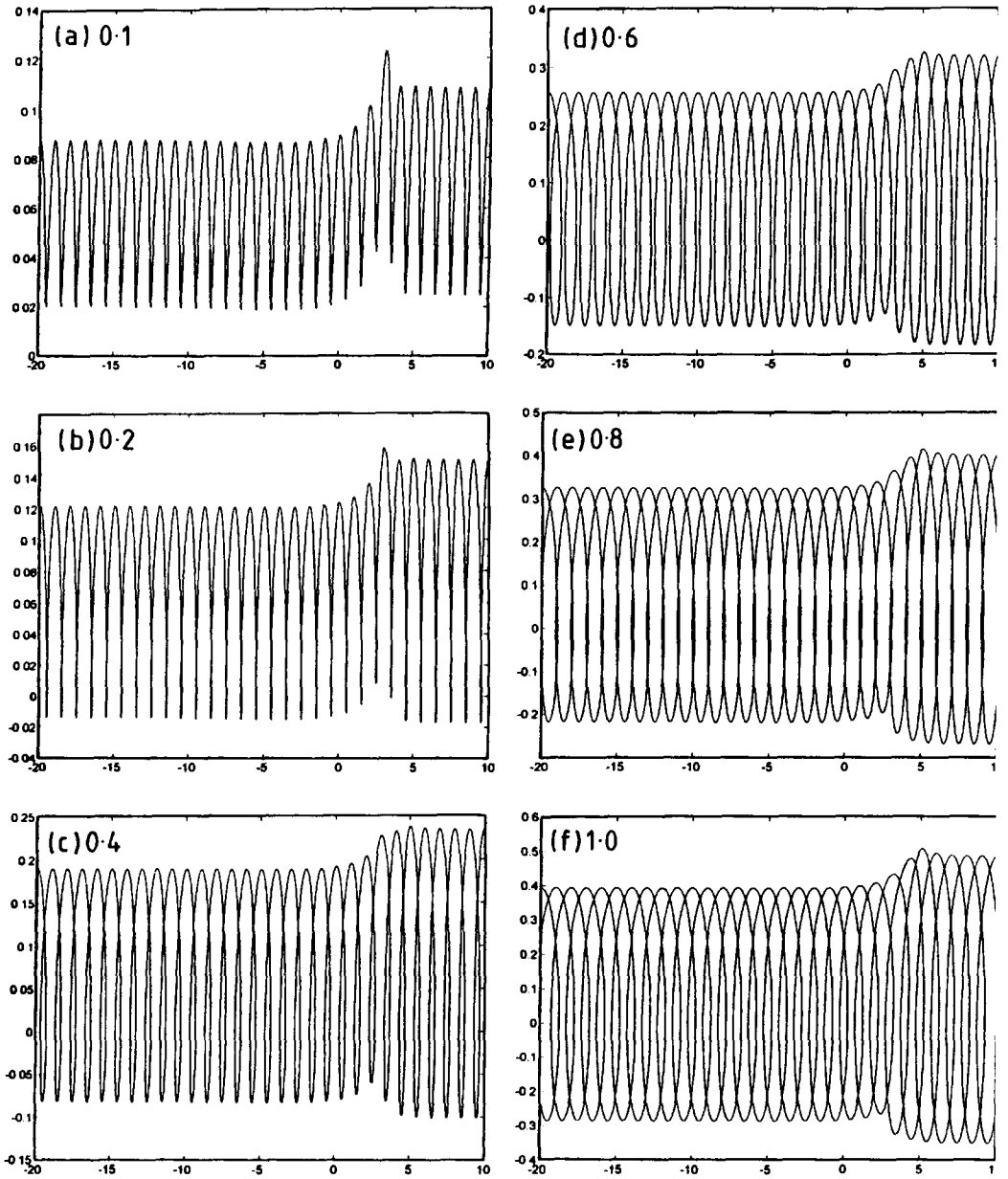

Fig. 16. Effect of amplitude of temperature modulation on heat flow in MDSC cycles with per = 24 s, $q_{av} = 2.5\,K\,min^{-1}$, $\delta_o = 6\,J\,g^{-1}$, and $x = 0.4$. The values of A_T are: (a) 0.1 K; (b) 0.2 K; (c) 0.4 K; (d) 0.6 K; (e) 0.8 K; (f) 1.0 K. All axes are: ordinates, heat flow in units of $W\,g^{-1}$; abscissae, $T - T_g$ in K.

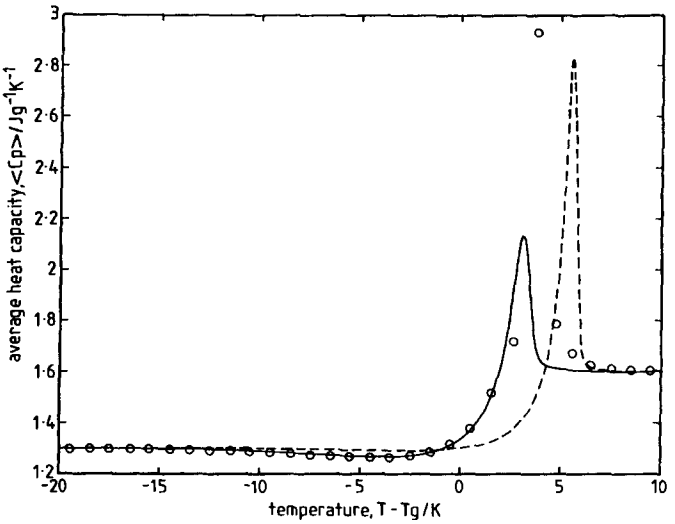

Fig. 17. Comparison of $\langle C_p \rangle$ from MDSC (circles) for which per = 24 s, $q_{av} = 2.5\,\mathrm{K\,min^{-1}}$, $\delta_o = 6\,\mathrm{J\,g^{-1}}$, $x = 0.4$ and $A_T = 1.0\,\mathrm{K}$, with C_p from conventional DSC: full line with $q = 2.5\,\mathrm{K\,min^{-1}}$; dashed line with $q = 18.2\,\mathrm{K\,min^{-1}}$.

mately linear scaling of the excess enthalpy response, as shown in Fig. 18. Until the response starts looping, at about $T - T_g = 3.5\,\mathrm{K}$, the 0.25 and 0.5 K MDSC responses pass through the conventional DSC response at approximately the same temperature, and in between these cross-over points the 0.5 K response departs from the conventional DSC response by approximately twice the departure of the 0.25 K response. The looping occurs primarily because the relaxation time τ, in the region where $\delta \approx 0$ for the conventional DSC, is not small in comparison with the period, so that the response passes from negative δ through equilibrium ($\delta = 0$) to positive values of δ, giving a kind of hysteretic effect.

Because the amplitude A_T appears to have this simple scaling effect, provided that it remains less than a critical limiting value, it has rather little effect on the other derived MDSC quantities. Interestingly, though, the maximum amplitude of the phase angle ϕ decreases slightly as A_T is increased, and positive phase angles appear before the usual negative values in the same MDSC scan for the smallest amplitudes used here. This is illustrated in Fig. 19 for selected values of A_T. The same effect is seen in the dependence of the loss heat capacity C_p'' on A_T, since C_p'' and ϕ are directly related for small angles ϕ (see Eq. (19)). The storage heat capacity C_p', on the other hand, is very insensitive to A_T for all but the smallest amplitudes (0.05 K here), and T_{mid} is independent of A_T.

3.3.4. *Effect of initial enthalpy*

The value of $\delta_o = 6\,\mathrm{J\,g^{-1}}$ that has been used for all the illustrations above is equivalent to an infinitely rapid quench from equilibrium at $T - T_g = 0$ to

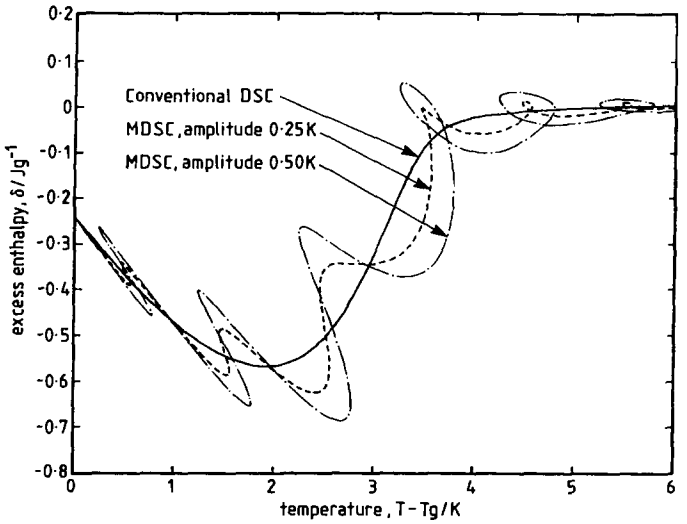

Fig. 18. Expanded view of the excess enthalpy modulation shown in Fig. 2 for MDSC cycles with per = 24 s, $q_{av} = 2.5$ K min^{-1}, $\delta_o = 6$ J g^{-1}, $x = 0.4$ and two different values of A_T: dashed line, 0.25 K; dash-dotted line, 0.5 K. Also shown (full line) is the conventional DSC response. Only the temperature interval from $T - T_g = 0$ to 6 K is shown in order to magnify the modulations.

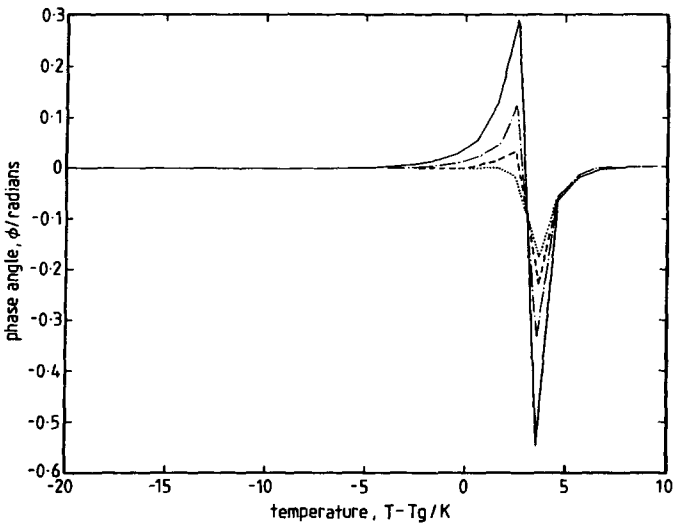

Fig. 19. Variation of phase angle with temperature for MDSC cycles with per = 24 s, $q_{av} = 2.5$ K min^{-1}, $\delta_o = 6$ J g^{-1}, $x = 0.4$ and the following values for A_T: full line, 0.05 K; dash-dotted line, 0.1 K, dashed line, 0.2 K; dotted line, 0.4 K. For clarity, the individual points have been omitted from these curves, and have simply been joined by straight lines.

$T - T_g = -20$ K. This is also close to the value (approximately 6.5 J g^{-1}) that is obtained at $T - T_g = -20$ K on cooling at -20 K min^{-1} from equilibrium at $T - T_g = 10$ K, with no modulation and for $x = 0.4$. A larger value of δ_0 would be equivalent to cooling at a faster rate than -20 K min^{-1}, while smaller values would result either from cooling at a slower rate or from increased periods of isothermal relaxation at $T - T_g = -20$ K. Since the present analysis involves only a single parameter model, there is no memory effect, and it is therefore only the value of δ_0, and not the thermal history required to achieve that value, which determines the subsequent DSC or MDSC scan on heating.

The effect of decreasing δ_0 from 7 to 5.5 J g^{-1} on the average heat capacity $\langle C_p \rangle$ is illustrated in Fig. 20. The increasingly large dip in the curves as δ_0 is increased represents the reduction in enthalpy that occurs on heating a glass for which the initial state was one of large excess enthalpy. The movement of the endothermic peak to higher temperatures as δ_0 decreases, i.e. on increased annealing at T_0, is expected, and would continue if δ_0 were reduced further below 5.5 J g^{-1}. For the single-parameter model used here, however, reduction in δ_0 much below 5.5 J g^{-1} leads to such a highly autocatalytic approach of the excess enthalpy towards equilibrium that the heat flow modulations display a spike (see Fig. 21). The meaning of a Fourier transformation of such data is dubious, and indeed gives rise to a phase angle ϕ which is, at its peak, more than $\pi/2$, resulting in negative values for C'_p. This problem would not occur in a multi-parameter model of MDSC, since the response would be much more distributed.

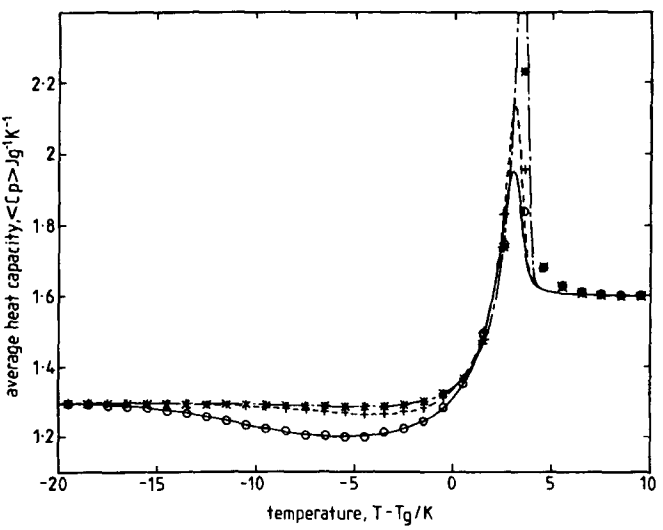

Fig. 20. Variation of the average specific heat capacity $\langle C_p \rangle$ as a function of temperature during MDSC cycles with per = 24 s, $A_T = 0.5$ K, $q_{av} = 2.5$ K min^{-1}, $x = 0.4$ and with different values of δ_0: ○, $\delta_0 = 7$ J g^{-1}; +, $\delta_0 = 6$ J g^{-1}; *, $\delta_0 = 5.5$ J g^{-1}. The full, dashed and dash-dotted lines represent, respectively, the response of the same model to conventional DSC with the same parameter values.

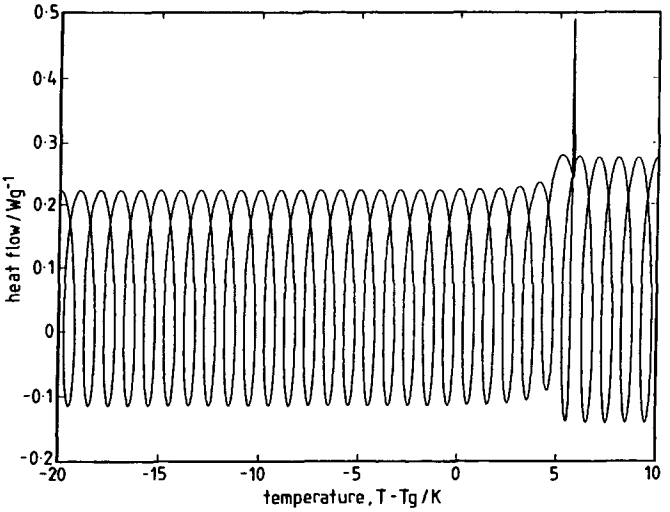

Fig. 21. Variation of heat flow with temperature in MDSC cycles with per = 24 s, $A_T = 0.5$ K, $q_{av} = 2.5$ K min^{-1}, $x = 0.4$ and $\delta_o = 4.5$ J g^{-1}.

With decreasing values of δ_o, the phase angle ϕ shows a maximum departure which increases gradually and moves to higher temperatures, whilst the temperature interval in which the departure from zero occurs becomes increasingly narrow. This is shown in Fig. 22 for the parameter values given in the caption. The loss specific heat capacity

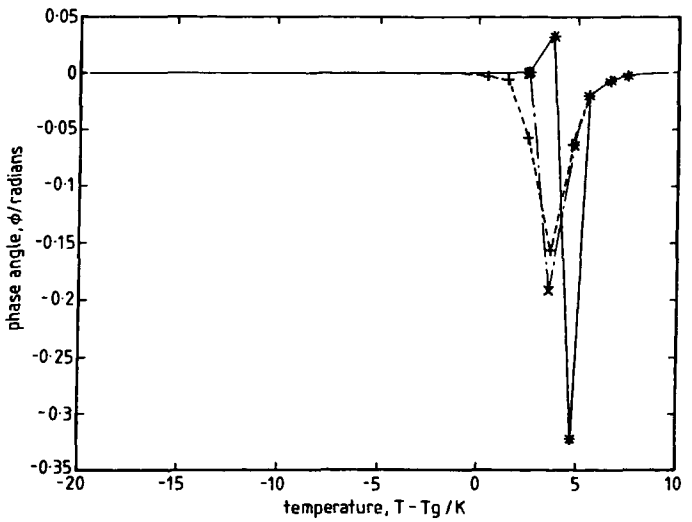

Fig. 22. Variation of phase angle ϕ with temperature for MDSC cycles with per = 24 s, $A_T = 0.5$ K, $q_{av} = 2.5$ K min^{-1}, $x = 0.4$ and with the following values for δ_o: +, 6.0 J g^{-1}; x, 5.5 J g^{-1}; *, 5.0 J g^{-1}. The lines are drawn through the points only to guide the eye.

C_p'' shows very similar behaviour, and shows the same trends as those observed in conventional DSC where the endothermic peak becomes increasingly sharp and moves to higher temperatures as δ_0 decreases.

Interestingly, the storage specific heat capacity C_p' shows very little change in the usual sigmoidal transition from glassy to liquid-like behaviour until $\delta_0 = 5.0\,J\,g^{-1}$. For this value of δ_0, a distinct peak in C_p' appears superimposed upon the sigmoid, as shown in Fig. 23, while the mid-point temperature has been shifted to slightly higher temperatures and the transition appears a little sharper. The difference of $1.0\,J\,g^{-1}$ between this value of δ_0 and the usual value of $6.0\,J\,g^{-1}$ used in the earlier illustrations (and also shown in Fig. 23) is equivalent to only a small amount of annealing in practice. For example, in epoxy resin annealed at $T - T_g = -20\,K$ approximately, an enthalpy loss of $1.0\,J\,g^{-1}$ occurs after only about 3 h [20]. Within reasonable experimental timescales, much greater enthalpy losses can be achieved; for example the same epoxy shows an enthalpy loss of $3.0\,J\,g^{-1}$ after some 1000 h at $T - T_g = -20\,K$. One might surmise that reducing δ_0 below $5.0\,J\,g^{-1}$ in the present calculations would lead to an increasingly pronounced peak in C_p' (Fig. 23) at increasingly higher temperatures, but the analysis must await the introduction of the multi-parameter model.

3.3.5. *Effect of the non-linearity parameter*

The non-linearity parameter x ($0 \leq x \leq 1$) controls the relative contributions of temperature and structure (δ or T_f) to the relaxation time (Eqs. (13) and (14)), with

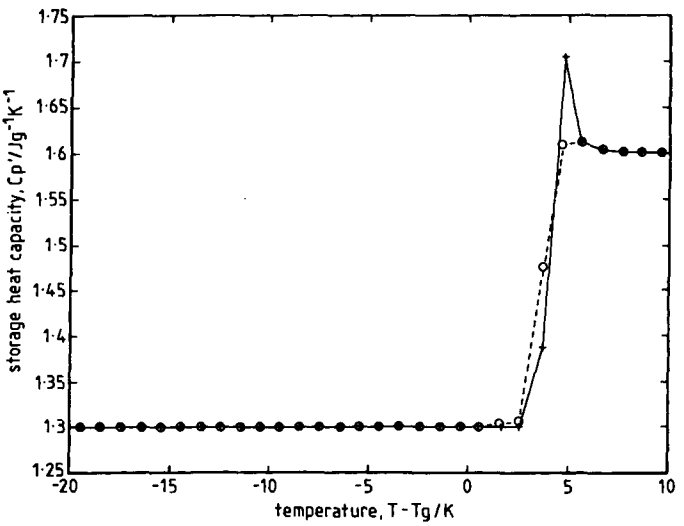

Fig. 23. Variation of storage heat capacity C_p' with temperature during MDSC cycles with per = 24 s, $A_T = 0.5\,K$, $q_{av} = 2.5\,K\,min^{-1}$, $x = 0.4$ and two values of δ_0: $6.0\,J\,g^{-1}$ (circles and dashed line) and $5.0\,J\,g^{-1}$ (crosses and full line). The lines are drawn only to guide the eye.

increasing non-linearity occurring as x approaches zero. Thus the effect of decreasing x on the average heat capacity $\langle C_p \rangle$ is to lead to increasing peak maximum values at increasing peak temperatures, and particularly so in the lower range of x values (0–0.3). This is very similar to the application of this model to conventional DSC, and indeed the results for $\langle C_p \rangle$ and C_p for conventional DSC are essentially the same for all values of x, except for the slight discrepancy noted earlier in the region of the endothermic peak and just above.

There is also a remarkable similarity between the effects of x and δ_0 on the phase angle ϕ (and on the loss specific heat C_p''). In particular, at low and decreasing values of x the phase angle departs more and more from zero, and the departure becomes increasingly sharp (compare the effect of δ_0 in Fig. 22). This similarity between the effects of x and δ_0 is not surprising in that decreasing each of them results in increasingly autocatalytic behaviour. Indeed, for the lowest value of x used here ($x = 0.1$), the heat flow modulations display a spike, just like that in Fig. 21, which results from an exceedingly rapid relaxation of enthalpy towards equilibrium, as shown in Fig. 24. The almost overlapping enthalpy modulations in the temperature range up to about $T - T_g = 6$ K indicate a virtually glassy response, with a slope very close to the glassy value of $C_{pg} = 1.3\,\mathrm{J\,g^{-1}K^{-1}}$. Suddenly, at about $T - T_g = 6.8$ K, the enthalpy relaxes to equilibrium, and thereafter the enthalpy modulations are entirely overlapping, as the structure follows the temperature modulations in the temperature range for which τ is much less than the period of the cycles. The slope of the line in this temperature interval gives the liquid-like specific heat capacity, $C_{pl} = 1.6\,\mathrm{J\,g^{-1}K^{-1}}$.

The effect of x on the storage heat capacity C_p' is small, with T_{mid} increasing only slightly as x decreases.

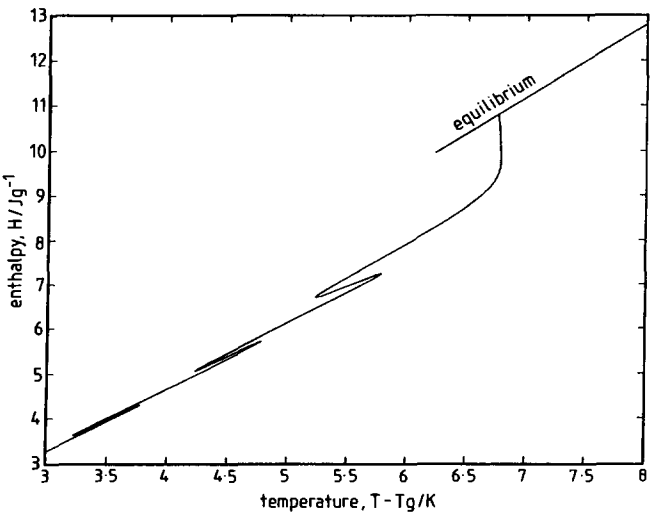

Fig. 24. Variation of enthalpy with temperature in the expanded range from $T - T_g = 3$ to 8 K for MDSC cycles with per = 24 s, $A_T = 0.5$ K, $q_{av} = 2.5\,\mathrm{K\,min^{-1}}$, $\delta_0 = 6\,\mathrm{J\,g^{-1}}$ and $x = 0.1$.

4. Discussion

The results presented above show a number of important aspects. First and foremost, the theoretical model here is able to describe, both qualitatively and to a certain extent quantitatively, the usual features observed by MDSC in the glass transition region. These features include: (i) the average heat capacity $\langle C_p \rangle$ is closely equivalent to the C_p obtained by conventional DSC at the constant average heating rate; (ii) the storage heat capacity C'_p or the reversing component usually shows a sigmoidal change from glassy to liquid-like behaviour in a temperature range around T_{mid} which increases with decreasing period of the modulations; (iii) the loss heat capacity C''_p and the phase angle both display a more or less abrupt departure from zero in the same temperature range around T_{mid}, with the maximum phase angle departure often being of the order of one or two tenths of a radian. This is believed to be the first time that these features of MDSC in the glass transition region have been described theoretically.

It must be pointed out, however, that both the theoretical model and the experimental MDSC technique employ a Fourier transformation procedure in order to analyse the data; this approach merits some further consideration.

First, any Fourier transformation must be based upon a linear response. Strictly speaking, the glass transition involves inherently non-linear kinetics, which may be characterised through the non-linearity parameter x introduced in Eqs. (13) and (14). However, provided that the amplitude of the temperature modulation is "small", the kinetic response will be approximately linear; the question is, what is the magnitude of this limiting "small" temperature modulation? There is no simple answer to this question, as it will depend upon other parameters of the system, and particularly on the value of x and on the period of the modulation cycles.

The importance of recognising this problem of non-linearity was illustrated in the results presented above, where for temperature amplitudes greater than about 0.6 K differences between the conventional and modulated DSC average C_p values appeared (see, for example, Fig. 17). There are, however, several results reported in the literature for which the temperature amplitudes might well exceed the limits of linear response: Wunderlich et al. [7] quote a temperature amplitude of 7.5 K; Schawe [6, 22] uses amplitudes of 1.0 K in both heating and cooling, using a sinusoidal modulation in a specially modified Perkin-Elmer DSC-7; Schawe also finds [23] for both simulated and experimental data for polystyrene and polyethylene terephthalate that larger amplitudes (in the range 1–7 K with periods of approximately 24 s) lead to broader heat capacity steps at the glass transition, but concludes that the amplitude must be as large as 5 K before it has any effect on the shape of the curve for storage heat capacity; and finally, Boller et al. [24] have investigated the ageing behaviour of polystyrene by MDSC using $A_T = 1.0$ K, as well as studying the effect of amplitudes up to 10 K, where a broadening is reported when the amplitude exceeds the inherent breadth of the transition region.

The amplitude of the modulation can clearly, therefore, be a complicating effect in the analysis, in that it may introduce non-linearity to the response. Even if this problem were to be overlooked, however, the fundamental question of the validity of the Fourier

transformation procedure must be addressed. It is clear from Fig. 3c that at temperature below (glassy region) and above (liquid-like region) the transition region, the heating rate and the heat flow are in phase; it is in the transition interval that the heat flow and the heating rate show a displacement relative to each other on the time scale, and this is evident also from experimental data. The interpretation that the heat flow and heating rate are simply out of phase in this region may, however, be questionable. Schawe's analysis [6] in terms of a complex specific heat capacity C_p^* and phase angle ϕ is in analogy with dynamic mechanical analysis (DMA) in which the stress and strain are out of phase by a phase angle δ, resulting in a complex modulus E^*. In DMA, though, if the structure of the sample remains constant, for example in isothermal operation, then the phase angle δ also remains constant, and may be meaningfully evaluated from a comparison of several stress and strain cycles. Even in constant heating rate mode, since the frequencies employed in DMA are usually much greater than those used in MDSC (typical frequencies in DMA range from 0.1 to 100 Hz giving periods shorter than 10 s, whereas MDSC periods are usually longer than 20 s), the structure of the sample may reasonably be assumed to remain constant over several cycles, though care must obviously be taken in this interpretation when low frequencies are used. In MDSC, the structure of the sample does not strictly remain constant in the transition interval; indeed this is the very reason why there is a transition. Hence, if the meaning of a phase angle ϕ is to be interpreted in any simple way, the experimental parameters must be chosen to ensure that the structural change of the sample per cycle is negligible. This may be difficult to accommodate with "heating only" cycles.

Assuming, however, that the data may be analysed in terms of a phase shift ϕ, one must then resolve the problem of how to determine its value. In other words, over how many cycles or over what portion of a single cycle should the heating rate and heat flow modulations be compared? The present model, being based upon a single relaxation time, obviously gives rather abrupt changes in the transition region, visible for example in Fig. 3c as the heat flow going out of phase and then back in phase with the heating rate again over only two cycles. In reality, the response will be much broader than this (and could be modelled by the multi-parameter KAHR model), but the same question still remains. The results obtained here using the single parameter model were derived from a consideration of only the fundamental frequency ω, in other words the first harmonic, of the heat flow modulations, ignoring the higher harmonics, and from successive single cycles of heating rate and the correspnonding heat flow values. This must introduce an averaging of the phase angle, which will vary even during a single cycle. Interpretation of the phase angle should therefore be made rather carefully in the light of the number of cycles over which the Fourier transformation is made. Current commercial practice is to use, as here, a single cycle of the heating rate.

In addition to the general features of MDSC response described above, the present model also allows a more detailed examination of the effects of several experimental and material parameters, for which the results have been discussed. In particular, this theory enables us to make a number of predictions of these effects, which are now considered.

One common feature that is predicted to occur, to a greater or lesser extent depending upon the combination of parameter values, is a small peak in the storage heat capacity C'_p (see, for example, Fig. 6). This peak is usually rather small, less than about 5% of the total specific heat capacity increment at the glass transition, and probably for this reason has never explicitly been remarked in published experimental data from MDSC studies. Nevertheless, there is evidence for its existence if reported data are examined carefully, as the following examples show: Fig. 5 in Ref. [2]; Fig. 5 in Ref. [3]; Fig. 3 in Ref. [24]. Similar peaks, though often of a rather larger magnitude, up to 10% or 20% of the heat capacity increment, are seen in conventional DSC scans on unannealed glasses, and have been referred to as "upper peaks" [25].

The principal effect of the average heating rate is on the average heat capacity $\langle C_p \rangle$. The prediction of the model is that $\langle C_p \rangle$ closely mirrors the C_p found by conventional DSC. This is the usual assumption, and indeed there are many examples of experimental data showing qualitative agreement, but a definitive quantitative assessment remains to be made.

A further prediction is that increasing q_{av} results in the phase angle displaying both positive and negative departures from zero, with corresponding changes in the loss heat capacity C''_p, whilst the storage heat capacity C'_p develops a more pronounced peak of the kind discussed above. There is very little published data regarding the phase angle, but there is some evidence from the data of Reading et al. [10] that, for $q_{av} = 3\,\mathrm{K\ min^{-1}}$, ϕ decreases initially before passing through a maximum and then returning towards its pre-transition value (compare the results shown in Fig. 19 for the effect of modulation amplitude).

The predominant effect of the period of the modulation is a shift of the mid-point temperature, T_{mid}, of the sigmoidal change in C'_p to higher temperatures as the period is reduced. This shift occurs both on heating and on cooling in MDSC, and has now been verified experimentally. For example, Schawe [22] finds for polystyrene a change of 2.6 K per decade on cooling, corresponding to an apparent activation energy of 1025 kJ mol^{-1}. On heating, the same author [23] finds, again for polystyrene, a slight non-linearity in the dependence of reciprocal temperature on log(frequency), but a best-fit straight line gives an apparent activation energy of 765 kJ mol^{-1}. It is interesting to note that our model predictions do not show the same difference in the apparent activation energy derived from heating and cooling MDSC experiments (see Fig. 14), with the former yielding the higher value, contrary to the observations of Schawe. Furthermore, earlier experimental results obtained for polystyrene by using conventional DSC [26,27] gave an apparent activation energy of 578 kJ mol^{-1} or 665 kJ mol^{-1}, lying below both of the values obtained by Schawe, but considerably less than the value obtained on cooling.

The results of Boller et al. [24] for polystyrene also show an increase in the transition temperature for the reversing component as the period is reduced, indicating a change of approximately 3 K when the period changes from 99 to 30 s, equivalent to an apparent activation energy of approximately 440 kJ mol^{-1}. (This value of 3 K is taken from their Fig. 4. In their text, Boller et al. report a change of only 2 K, which would lead to a larger apparent activation energy, approximately 690 kJ mol^{-1}.) It should be

noted, though, that these experiments were made in a "quasi-isothermal" mode, at a sequence of 24 temperatures during cooling from 400 to about 340 K; without any indication of cooling rates or annealing periods, it is not possible to identify the all-important structural state of the sample in these experiments, a state that would have been defined precisely if the normal MDSC mode, in either cooling or heating, had been used.

The effect of the amplitude of temperature modulation is predicted here to be rather small in general, and experimental data confirm this [23, 24], though a slight broadening of the transition region, identified by C'_p or the reversing component, is seen when large amplitudes (5–10 K) are used. The prediction of the small effect on the phase angle ϕ (see Fig. 19), and correspondingly on C''_p, has not been reported experimentally.

Systematic studies of the effects of enthalpy relaxation, in other words of the effect of the initial enthalpic state before the MDSC heating scan, are very limited. For polystyrene, Boller et al. [24] show how the reversing heat capacity moves to slightly higher temperatures and the transition becomes a little sharper as longer annealing times at temperatures decreasing within the transition interval are used, though the enthalpy changes due to these annealing treatments are not quantified. Interestingly, this is similar to the behaviour predicted by the present model for the phase angle (see Fig. 22), but a more direct comparison would be preferable.

In this context, in particular, the question of what the loss heat capacity C''_p, or indeed the non-reversing heat capacity, actually means physically remains somewhat elusive. It is well known that the difference in enthalpy between two states A and B can be obtained by conventional DSC as the difference between the areas under the C_p traces obtained on heating at constant rate from each of the states A and B until equilibrium is achieved at a temperature above the transition region. If there is a change in the area under the reversing C_p trace as the initial enthalpic state changes, as is suggested by the results of Boller et al. [24], then the change in the area under the non-reversing C_p (recall that the non-reversing component is simply the difference between the total and reversing components) cannot simply represent the enthalpy change.

The situation is more difficult to rationalise for C''_p. The appearance of a peak in C''_p certainly does not, in itself, signify that enthalpy relaxation has occurred. This is evident from the fact that a peak in C''_p occurs on cooling in MDSC as well as on heating. This has been noted earlier by Schawe [6] and also emerges from the present theoretical model, as is shown in Fig. 25. The departure of C''_p from zero arises because the phase angle departs from zero, which itself results simply from the relaxation kinetics. Indeed, integration of the C''_p traces, such as that shown in Fig. 7, reveals no significant change in the area when δ_0 reduces by 2 J g^{-1} from 7 to 5 J g^{-1}. Although it is difficult to make a precise evaluation of these areas as the C''_p traces are composed of discrete data points (in this case at 1 K temperature intervals), it appears that the area remains essentially constant at 0.45 ± 0.1 J g^{-1} under these conditions, well below the actual 2 J g^{-1} enthalpy change.

A clearer picture of this and the other aspects discussed above may emerge from a multi-parameter model treatment of MDSC, and work on this is currently in progress.

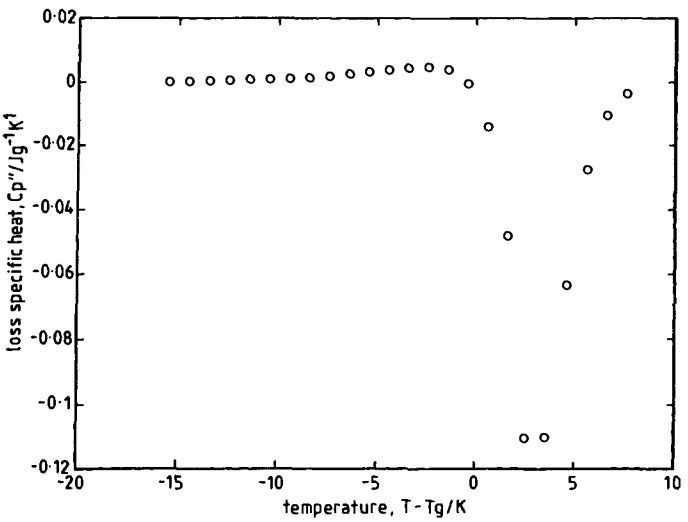

Fig. 25. Dependence of loss specific heat on temperature during cooling for MDSC cycles with per = 24 s, $A_T = 0.25$ K, $\delta_o = 0$ J g^{-1} at $T - T_g = 8$ K, $x = 0.4$ and $q_{av} = -2.5$ K min^{-1}.

5. Conclusions

A theoretical model, based upon a single relaxation time, has been used to describe the response of glasses to the sinusoidally varying heating rate of modulated differential scanning calorimetry. The theoretical curves for heat flow are analysed using the complex specific heat capacity approach.

The model describes semi-quantitatively all of the usually observed features of MDSC, namely: (i) the average or total specific heat capacity from MDSC is very similar to the conventional DSC output for the same average heating rate; (ii) the phase angle ϕ and the loss specific heat C_p'' show a peak in the transition region, the former with a maximum departure from zero of typically 0.1 or 0.2 radians; (iii) the storage heat capacity C_p' shows an essentially sigmoidal change from glassy to liquid-like values. This is the first time that these features have been predicted quantitatively.

The model further allows predictions to be made of the effects of the experimental and material parameters. The average heating rate of MDSC is shown to have a significant effect only on the average or total C_p, following the same dependence as for conventional DSC. Of the other parameters, the dominant effect is that of the period of the cycles, with the sigmoidal transition in C_p' occurring at higher temperatures the shorter the period. A similar effect is seen also on cooling in MDSC, but the temperature changes appear to be slightly different from those found on heating.

The amplitude of the temperature modulations, at least for reasonable values up to about 0.6 K, appears to have no significant effect on the MDSC-derived quantities, since it results in an approximately linear scaling of the excess enthalpy response.

The effect of the initial enthalpic state δ_o on the average C_p is very similar to that for conventional DSC. With decreasing values of δ_o, the phase angle and C_p'' both show

increasingly large departures from zero centred at increasing temperatures. The effect on C'_p is little, though a small peak does appear superimposed on the sigmoidal change at the end of the transition for the lowest value of δ_0 used here. The effect of the non-linearity parameter x appears rather similar to that of δ_0.

The physical meaning of C''_p, particularly in the context of MDSC studies of glasses annealed below the glass transition region, remains unclear, but it cannot be attributed simply to enthalpy relaxation.

Further refinement of this analysis requires the application of the multi-parameter model, in particular so that memory effects can be included. This development will also permit a better Fourier transformation of the heat flow modulations, since it will smooth out the rather abrupt changes inherent in the simpler single-parameter model used here. Work in this direction is currently in progress.

Acknowledgements

JMH is grateful to the University of Aberdeen for permission to take leave of absence, to the Generalitat de Catalunya for the provision of a grant, and to the Universitat Politècnica de Catalunya, Terrassa, for their hospitality. Financial support has been provided by the DGI CYT (Project no. PB 43/1421).

References

[1] J.C. Seferis, I.M. Salin, P.S. Gill and M. Reading, Proc. Acad. Greece, 67 (1992) 311.
[2] P.S. Gill, S.R. Sauerbrunn and M. Reading, J. Therm. Anal., 40 (1993) 931.
[3] M. Reading, D. Elliott and V.L. Hill, J. Therm. Anal., 40 (1993) 949.
[4] M. Reading, B.K. Hahn and B.S. Crowe, United States Patent 5, 224 775 (1993).
[5] J.M. Hutchinson, M.T. Clavaguera Mora, J. Zhu and S. Montserrat, Part II of this series, Thermochim. Acta, to be submitted.
[6] J.E.K. Schawe, Thermochim. Acta, 260 (1995) 1.
[7] B. Wunderlich, Y. Jin and A. Boller, Thermochim. Acta, 238 (1994) 277.
[8] A. Boller, Y. Jin and B. Wunderlich, J. Therm. Anal., 42 (1994) 307.
[9] M. Reading, Trends Polym. Sci., 18 (1993) 248.
[10] M. Reading, A. Luget and R. Wilson, Thermochim. Acta, 238 (1994) 295.
[11] N. Hirai and H. Eyring, J. Appl. Phys., 29 (1958) 810.
[12] N. Hirai and N. Eyring, J. Polym. Sci., 37 (1959) 51.
[13] A.J. Kovacs and J.M. Hutchinson, J. Polym. Sci., Polym. Phys. Edn., 17 (1979) 2031.
[14] A.J. Kovacs, J.J. Aklonis, J.M. Hutchinson and A.R. Ramos, J. Polym. Sci., Polym. Phys. Edn., 17 (1979) 1097.
[15] A.J. Kovacs, J.M. Hutchinson and J.J. Aklonis, P.H. Gaskell (Ed.), The Structure of Non-Crystalline Materials, Taylor and Francis, London, 1977, p. 153–163.
[16] A.Q. Tool, J. Am. Ceram. Soc., 29 (1946) 240.
[17] O.S. Narayanaswamy, J. Am. Ceram. Soc., 54 (1971) 491.
[18] C.T. Moynihan, A.J. Easteal, M.A. DeBolt and J. Tucker, J. Am. Ceram. Soc., 59 (1976) 12.
[19] J.M. Hutchinson, M. Ruddy and M.R. Wilson, Polymer, 29 (1988) 152.
[20] S. Montserrat, P. Cortés, A.J. Pappin, K.H. Quah and J.M. Hutchinson, J. Non-Cryst. Solids, 172–174 (1994) 1017.
[21] J.M. Hutchinson, unpublished results (1995).

[22] J.E.K. Schawe, Thermochim. Acta, 261 (1995) 183.
[23] J.E.K. Schawe, Thermochim. Acta, submitted.
[24] A. Boller, C. Schick and B. Wunderlich, Thermochim. Acta, 266 (1995) 97.
[25] J.M. Hutchinson and M. Ruddy, J. Polym. Sci., Polym. Phys. Edn., 28 (1990) 2127.
[26] J.M. Hutchinson and M. Ruddy, J. Polym. Sci., Polym. Phys. Edn., 26 (1988) 2341.
[27] I.M. Hodge, Macromolecules, 20 (1987) 2897.